Towards Magnetic Field Energy Harvesting near Electrified Railway Tracks

Asbjørn Engmark Espe
Department of Engineering Cybernetics,
Norwegian University of Science and Technology,
Trondheim, Norway
E-mail: asbjorn.e.espe@ntnu.no

Geir Mathisen
Department of Engineering Cybernetics,
Norwegian University of Science and Technology,
Trondheim, Norway
E-mail: geir.mathisen@ntnu.no

***Abstract*—This paper evaluates the feasibility of magnetic field energy harvesting (MFEH) near electrified railway tracks, for the purpose of increasing the lifetime of distributed condition monitoring systems. Since MFEH is a novel concept for railway applications, relevant previous work from a power grid context is employed. Using a theoretical model along with simulations, it is estimated that the power output of a solenoid placed near the return current may be sufficient for a monitoring system designed for low-power operation and low-duty-cycle wireless communication. The magnetic induction is estimated to be at least 25 µT at a distance of 0.5 m from the closest rail, and it is argued that an efficient induction energy harvester placed in this magnetic field could potentially increase the lifetime of condition monitoring systems indefinitely.**

***Index Terms*—Energy harvesting, railway, magnetic field, condition monitoring.**

I. Introduction

Permeating a wide range of industries, *in situ* condition monitoring systems have become a pervasive part of modern society. For the railway industry in particular, it is desirable to install trackside systems for condition monitoring of infrastructure such as bridges, tracks, and tunnels in order to detect faults before they escalate [1]. This has become even more relevant in recent times as the effects of climate change become apparent, such as an increase in the frequency of extreme weather. For systems to be placed near electrified railway tracks, the railway electrification system may be directly utilised for system power. However, the supply voltage typically lies in the range of tens of kilovolts, which inherently makes any system to be powered by it expensive in terms of components and hazardous to deploy.

In later years, advances in technology have made inexpensive battery-powered wireless sensor networks feasible for condition monitoring. However, such systems require some method of acquiring energy in order to avoid the maintenance workload associated with battery replacement or charging [2]. Compared to systems directly utilising the railway power supply, a non-intrusive, low-maintenance energy harvesting solution would presumably lend itself to lower-cost construction and operation, as well as safer and simpler deployment—especially since access to the high-voltage contact line would not be required. Cost-effective construction and deployment would also allow for instrumentation at locations where such systems were previously economically infeasible.

For trackside railway equipment, several energy harvesting solutions can be found in the literature. The predominant energy source used in these systems has been vibration [3]–[5], though solar energy has also been explored [6]. Instances of magnetic field energy harvesting (MFEH) for use in railway, however, could not be found in the literature. Nonetheless, much relevant research exists in the context of power grid transmission lines. Roscoe and Judd [7] describe a free-standing MFEH solution providing 300 µW on average. Yuan et al. [8] propose an efficient bow-tie solenoid core design which is able to harvest 360 µW from a 7 µT applied magnetic field. They subsequently improve this figure fourfold with a more complex helical core [9]. A small design in [10] is zip-tied to the power lines and able to harvest more than 30 mW, and proposed in [11] is a credit-card-sized coil with a flux guide that can harvest around 230 mW.

Mainline electrified railways can generally be organised into two classes depending on their traction power type: alternating current (AC) and direct current (DC) systems. MFEH is generally only possible for the former, as a time-varying flux is required for induction. Measured in length, 63 % of electrified railway lines worldwide operate using AC, with supply voltages of either 15 kV, 16 ⅔ Hz or 25 kV, 50 Hz being most common [12]. For practical reasons, this paper will target Norwegian railway, which employs the 16 ⅔ Hz system. Illustrated in Fig. 1 is the most common contact line configuration in Norway—

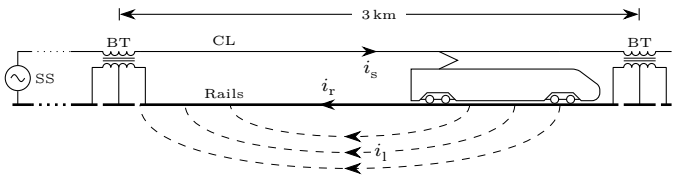

Fig. 1. *System B*—the most common return circuit employed in Norwegian railway. The supply current i_s from the substation (SS) is carried by the contact line (CL) and returned through the rails as i_r, and partly as leakage currents i_l through earth. Booster transformers (BT) are placed at regular intervals to minimise the leakage currents.

known as *System B* in Norwegian literature [13]. The system uses booster transformers, but lacks a dedicated return conductor [12]. This means that the supply current i_s from the contact line is returned as current i_r through the rails, as well as through ground leakage currents i_l. The booster transformers are placed at regular intervals—usually 3 km—in order to maximise the return current through the rails, and thus decrease i_l. At the point farthest from the booster transformers, it is estimated that about 7.5 % of the total return current is lost to leakage currents [13]. In other words, a substantial part of the current is carried by the rails, and may be utilised in MFEH for powering trackside systems.

II. Theoretical Model

A traditional current transformer (CT) design enclosing the current is not applicable since trains will be running on the rails. However, a solenoid may be placed in the vicinity of the rail to harvest energy from its surrounding magnetic field. For ease of installation, the solenoid will be mounted on the ground plane near the rails, i.e. it is assumed that the vertical centre of the solenoid will be on the same plane as the vertical centre of the rails.

A. Magnetic Field

In order to model the magnetic field surrounding the rails, some assumptions must be made. First, since the section of railway that carries current as the train passes may be several kilometres long, it can be assumed that the railway track is infinitely long compared to the dimensions of the solenoid. Furthermore, at a large enough radial distance from the current, the rail shape may be approximated as a cylinder. With these assumptions, a simple form of the Biot-Savart law (1) is employed to describe the magnetic field around the rail [14].

$$\mathbf{H} = \frac{i_\mathrm{r}}{2\pi r}\hat{\boldsymbol{\phi}} \tag{1}$$

The current gives rise to an approximately circular magnetic field as illustrated in Fig. 2. The figure shows the cross section of a rail with return current i_r and its surrounding magnetic field, with the potential placement of the energy harvesting solenoid highlighted.

The magnetic field described by (1) only accounts for a single rail. Fortunately, introducing a second rail to the model is quite simple through superposition. First, it is assumed that the dimensions of the solenoid are much less than its distance d_s away from the rail, which means that r may be regarded as a constant parameter in (1). The same assumption also allows the approximation $\hat{\boldsymbol{\phi}} \approx \hat{\mathbf{y}}$, which will bring the equation into Cartesian co-ordinates. Moreover, an inverse effective distance coefficient is defined as shown in (2), to account for the contribution of each rail, where d_rr denotes the distance between the two rails.

$$d_\mathrm{e} = \frac{1}{d_\mathrm{s}} + \frac{1}{d_\mathrm{s} + d_\mathrm{rr}} \tag{2}$$

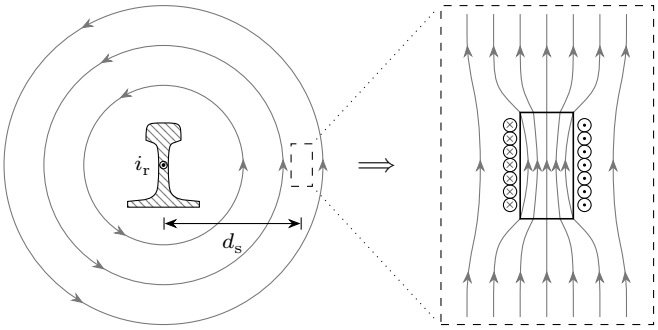

Fig. 2. A current-carrying rail will generate an approximately circular magnetic field. A solid-core solenoid may be placed in its vicinity to focus the field lines and harvest energy.

Assuming that each rail carries approximately half of the total return current, an expression for the total magnetic field strength at the position of the solenoid may be defined as shown in (3).

$$\mathbf{H}_0 = \frac{i_\mathrm{r} d_\mathrm{e}}{4\pi}\hat{\mathbf{y}} \tag{3}$$

Following from the assumptions in the previous, the magnetic field is close to uniform, and points in the positive $\hat{\mathbf{y}}$-direction.

B. Core Demagnetisation

The solenoid is constructed as a wire coiled around a solid core with relative permeability $\mu_\mathrm{r} > 1$. Since the solid-core solenoid does not enclose the rail, the generation of a magnetic dipole moment gives rise to a demagnetising field opposing the applied field $\mathbf{H}_0$. This means that the magnetic field $\mathbf{H}_\mathrm{s}$ in the solenoid core will be less than $\mathbf{H}_0$, and may be expressed as (4), where $\mathbf{M}_\mathrm{s}$ is the core's magnetisation, and N_d is the demagnetisation factor [14].

$$\mathbf{H}_\mathrm{s} = \mathbf{H}_0 - N_\mathrm{d}\mathbf{M}_\mathrm{s} \tag{4}$$

Under the assumption that the applied magnetic field is close to uniform and weak to the extent that the core's response is linear, the magnetic induction within the solenoid may be approximately described by the scalar expression $B_\mathrm{s} = \mu_\mathrm{e}\mu_0 H_0$, where μ_e is a measure of the core's *effective* permeability. A relation can be derived as shown in (5), which reveals that the effective permeability depends on the demagnetisation factor N_d, and will be in the range $1 \leq \mu_\mathrm{e} \leq \mu_\mathrm{r}$.

$$\mu_\mathrm{e} = \frac{\mu_\mathrm{r}}{1 + N_\mathrm{d}\left(\mu_\mathrm{r} - 1\right)} \tag{5}$$

N_d is mainly determined by core shape. For a cylinder, such as the one illustrated in Fig. 2, the demagnetisation factor is directly obtainable from its dimensions [14]. However, alternative core designs can considerably reduce N_d and thereby increase core efficiency. Examples in the literature include a U-shaped flux guide [11], a bow-tie shape [8], and a helical core [9].

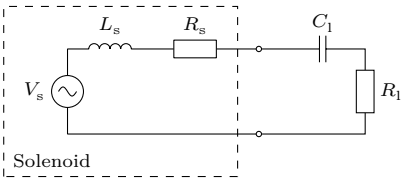

Fig. 3. Equivalent circuit of the magnetic field energy harvester.

C. Modelling losses

There are two additional loss mechanisms that may affect the solenoid's efficiency of a solenoid energy harvester: hysteresis loss and eddy current loss [14].

1) Hysteresis loss: The hysteresis losses account for the work done by a periodically reversing magnetic field in order to magnetise the core material. In this application, however, the frequency and magnitude of the magnetic induction are very low, which allows the material response to be considered linear.

2) Eddy current loss: Eddy currents can have a great impact on the efficiency of a solenoid energy harvester [7]. According to [14], the power loss in a cylinder stemming from eddy currents can be modelled using the expression shown in (6), where d is the diameter of the cylinder, f is the frequency, B_p is the peak magnetic induction, and ρ is the resistivity of the core material.

$$W_\mathrm{ec} = \frac{\pi^2 B_\mathrm{p}^2 d^2 f^2}{16\rho} \tag{6}$$

From this equation, it is evident that a higher resistivity and smaller-diameter core will reduce the losses.

D. Power output

As shown in (7), Faraday's law may be applied to determine the induced electromotive force in the solenoid.

$$\mathcal{E} = -N\frac{\mathrm{d}\Phi_\mathrm{s}}{\mathrm{d}t} = -N\frac{\mathrm{d}(B_\mathrm{s}A)}{\mathrm{d}t} = -NA\mu_\mathrm{e}\mu_0\frac{\mathrm{d}H_0}{\mathrm{d}t} \tag{7}$$

In the following, $\mathbf{I}_\mathrm{r}$ is introduced as a shorthand for the root-mean-square (RMS) phasor $I_\mathrm{r}\angle 0°$, and in time-domain equivalent to $i_\mathrm{r} = \sqrt{2}\,I_\mathrm{r}\cos(\omega t)$. Likewise, the value $\mathbf{V}_\mathrm{s}$ denotes the open-circuit voltage in the solenoid as an RMS phasor. Its sign depends on the coil winding direction, so for simplicity, it is defined as the negative of the electromotive force. Inserting the cross-sectional area $A = \pi r_\mathrm{s}^2$, as well as the applied magnetic field strength from (3) into (7), the relation between the return current and open-circuit voltage is obtained.

$$\mathbf{V}_\mathrm{s} = j\omega\frac{N\mu_\mathrm{e}\mu_0 d_\mathrm{e} r_\mathrm{s}^2}{4}\mathbf{I}_\mathrm{r} \tag{8}$$

According to the maximum power theorem, the power transfer is maximised when the load impedance is equal to the complex conjugate of the source impedance. The solenoid impedance is equivalent to an inductor in series with a resistor, which means that a matched load must have a resistance and compensating capacitance, as highlighted by the equivalent circuit in Fig. 3. It follows that

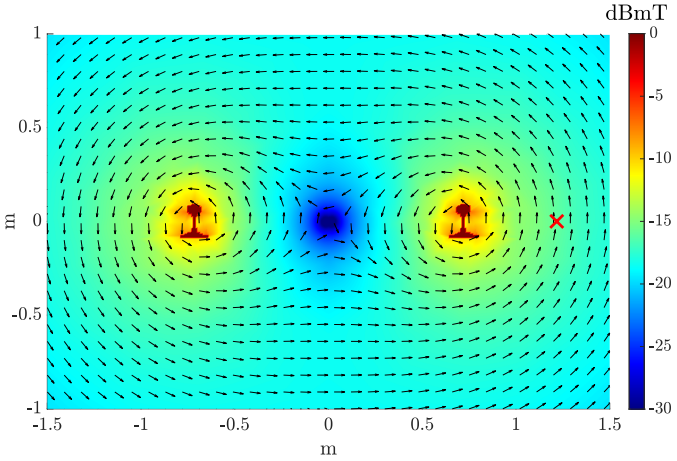

Fig. 4. The magnetic field around two *60E1*-type rails, simulated in *CST Studio 2019*.

for maximum efficiency, $R_\mathrm{l} = R_\mathrm{s}$ and $C_\mathrm{l} = \frac{1}{\omega^2 L_\mathrm{s}}$. As shown in (9), the solenoid's internal resistance is derived from the resistivity ρ of the wire material, its cross-sectional area A_w, and its length $2\pi N r_\mathrm{s}$.

$$R_\mathrm{s} = \frac{2\pi\rho N r_\mathrm{s}}{A_\mathrm{w}} \tag{9}$$

The active power delivered to the load is then derived as follows.

$$P_\mathrm{l} = \frac{|\mathbf{V}_\mathrm{s}|^2}{4R_\mathrm{s}} = \frac{\pi N A_\mathrm{w} r_\mathrm{s}^3}{32\rho}\left(\mu_\mathrm{e}\mu_0 d_\mathrm{e} f I_\mathrm{r}\right)^2 \tag{10}$$

The simplest approach towards increased power output seems to be core design, especially if it can affect both r_s and μ_e positively. The number of windings N can also be increased, but after a certain point, the thickness of the coil will make the expression (9) inaccurate. It may even require decreasing A_w, which will increase wire resistance.

III. Results and Discussion

In the following, 100 A RMS is employed as an estimate of the average current draw of a typical Norwegian passenger train with the common *Rc8* electric locomotive [15]. Fig. 4 shows a cross section of the simulated magnetic field generated by the return current in the rails, assuming each carries a current of 50 A. The rails are separated by a distance of $d_\mathrm{rr} = 1.435\,\mathrm{m}$, and are modelled pursuant to the standard *60E1* [16]—a common rail profile in Norway. The arrows show the direction of the field, while the colour designates the magnitude in decibels relative to 1 mT. The simulation reports the magnitude of magnetic induction as 25.0 µT at the red cross, which marks a potential location of the energy harvester, 0.5 m from the right rail. The theoretical model derived in Section II gives a magnetic induction of 25.2 µT at the same point, resulting in an error of 0.8 %. In fact, as shown in Fig. 5, the simulated magnetic induction is closely approximated by the theoretical model from a distance of about 0.4 m outwards.

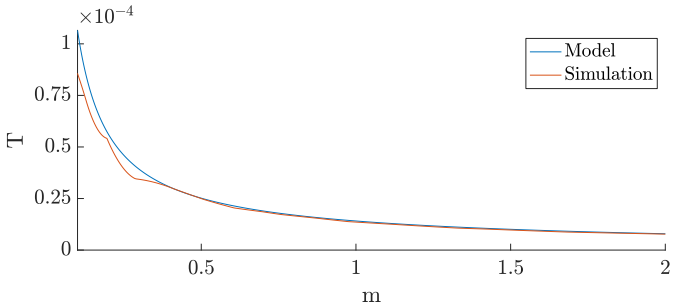

Fig. 5. The magnetic induction tapers off as the distance increases from the rail. The theoretical model closely approximates the simulated scenario.

As shown in (10), the power output in a typical energy harvester design scales with both frequency and current. While the results in this paper are based on Norwegian railways, operating at $16\,^2/_3\,\mathrm{Hz}$, the dependence on f^2 should mean an increase in output power for railways operating at 50 Hz. Moreover, the dependence on I_r^2 means that an increase in current will have a large effect on output power. The figure of 100 A used in the previous is in many cases a rather conservative estimate. While the current draw of a passenger locomotive can be as low as 50 A on flat railway segments, according to Olsen [15], certain freight trains may draw up to 900 A during acceleration, generating an estimated magnetic induction of 227 µT at 0.5 m. Furthermore, if multiple trains are running on the same track segment, each will contribute to the total return current.

For a cylindrical ferrite-core solenoid with radius 50 mm, length 150 mm, $\mu_\mathrm{r} = 250$, [14] reports a demagnetisation factor $N_\mathrm{d} = 0.18$, meaning an effective permeability of $\mu_\mathrm{e} = 5.46$. With 40 000 windings of a wire with total resistance 1.4 kΩ, the power output is estimated to be just 0.38 µW. However, using their novel bow-tie core design ($N_d = 0.007$), Yuan et al. [8] reported a power output of 360 µW in a magnetic field of merely 7 µT RMS. Their figure is sufficient to power a low-duty-cycle sensor system, which may require tens to hundreds of microwatts in active operation, and tens of nanowatts in *sleep*-mode [2]. Since the magnetic induction in railway is estimated to be at least 25 µT RMS, the conclusion is that MFEH in railway is feasible, but its power output depends heavily on core design.

A. Future Work

On the basis of theoretical modelling and simulations, MFEH in railway has been deemed feasible, which means the next step is to create a prototype and conduct tests *in situ*. In order to investigate the general availability of magnetic field energy, future research will involve empirical measurements of the magnetic field at different times and locations, as well as with varying amount of railway traffic on a track segment.

Different core designs should be explored, since the power output is highly dependent on an efficient core shape. Some designs specific to this application may be especially interesting—for instance a core that partially wraps around the rail to decrease demagnetisation.

IV. Conclusions

This paper set out to evaluate the feasibility of magnetic field energy harvesting in the vicinity of electrified railway tracks. Using an approximate model of the magnetic field, an expression for theoretical power output of a typical energy harvester was derived, and its output was shown to be heavily dependent on core design. Verified against simulations of the magnetic field, the model was found to be very accurate as distance from the rail increases. In comparison with similar cases in the literature, the magnetic induction near the rails is sufficient for energy harvesting, and should therefore be explored further.

References

[1] V. J. Hodge, S. O'Keefe, M. Weeks, and A. Moulds, "Wireless Sensor Networks for Condition Monitoring in the Railway Industry: A Survey," *IEEE Trans. Intell. Transp. Syst.*, vol. 16, no. 3, pp. 1088–1106, Jun. 2015.

[2] D. E. Boyle, M. E. Kiziroglou, P. D. Mitcheson, and E. M. Yeatman, "Energy Provision and Storage for Pervasive Computing," *IEEE Pervasive Comput.*, vol. 15, no. 4, pp. 28–35, Oct. 2016.

[3] M. K. M. Wischke, M. Masur and P. Woias, "Vibration harvesting in traffic tunnels to power wireless sensor nodes," *Smart Mater. and Struct.*, vol. 20, no. 8, p. 085014, Jul. 2011.

[4] J. J. Wang, G. P. Penamalli, and L. Zuo, "Electromagnetic energy harvesting from train induced railway track vibrations," in *Proc. 8th IEEE/ASME Int. Conf. on Mechatronic and Embedded Syst. and Appl.*, Suzhou, China, 2012, pp. 29–34.

[5] A. Pourghodrat, C. A. Nelson, S. E. Hansen, V. Kamarajugadda, and S. R. Platt, "Power harvesting systems design for railroad safety," in *Proc. of the Institution of Mech. Engineers, Part F: J. of Rail and Rapid Transit*, vol. 228, no. 5, 2014, pp. 504–521.

[6] A. L. Ruscelli, G. Cecchetti, and P. Castoldi, "Energy Harvesting for Trackside Railways Communications," in *11th World Congr. on Railway Res.*, Milan, Italy, 2016.

[7] N. M. Roscoe and M. D. Judd, "Harvesting Energy from Magnetic Fields to Power Condition Monitoring Sensors," *IEEE Sensors J.*, vol. 13, no. 6, pp. 2263–2270, Jun. 2013.

[8] S. Yuan, Y. Huang, J. Zhou, Q. Xu, C. Song, and P. Thompson, "Magnetic Field Energy Harvesting under Overhead Power Lines," *IEEE Trans. Power Electron.*, vol. 30, no. 11, pp. 6191–6202, Nov. 2015.

[9] S. Yuan, Y. Huang, J. Zhou, Q. Xu, C. Song, and G. Yuan, "A High-Efficiency Helical Core for Magnetic Field Energy Harvesting," *IEEE Trans. Power Electron.*, vol. 32, no. 7, pp. 5365–5376, Jul. 2017.

[10] W. Jiang, J. Lu, S. Hashimoto, and Z. Lin, "A non-intrusive magnetic energy scavanger for renewable power generation state monitoring," in *IEEE Int. Conf. on Renewable Energy Res. and Appl.*, Birmingham, UK, 2016, pp. 562–566.

[11] Z. Wu, D. S. Nguyen, R. M. White, P. K. Wright, G. O'Toole, and J. R. Stetter, "Electromagnetic energy harvester for atmospheric sensors on overhead power distribution lines," *J. of Phys.: Conf. Ser.*, vol. 1052, no. 1, Jul. 2018.

[12] F. Kiessling, R. Puschmann, A. Schmieder, and E. Schneider, *Contact Lines for Electric Railways*, 1st ed. Munich, Germany: Publicis, 2001.

[13] F. Nilsen, "Sporstrømmer og potensialer i kontaktledningsanlegg," Jernbaneverket, Tech. Rep., 1997, (in Norwegian).

[14] D. Jiles, *Introduction to Magnetism and Magnetic Materials*, 1st ed. London, UK: Chapman and Hall, 1991.

[15] B. I. Olsen, Bane NOR, Mar. 2020, personal communication.

[16] *Railway applications - Track - Rail - Part 1: Vignole railway rails 46 kg/m and above*, NS-EN 13674-1:2011+A1:2017, 2017.